Selectively Doped Zinc Oxide Polyscale Designer Particulates

Abstract

Hydrothermal synthesis of selectively doped zinc oxide (ZnO) polyscale designer particulates was carried out at temperatures 150 to 250^{o}C with an autogeneous pressure and experimental duration 12 to 40 hours. ZnO was selectively doped with Cr, Fe, Mn, Cd, Sn, In, Ag, Nd, Mo and W in different concentrations (1 to 5 w%). The molarity of ZnO was varied from 1M to 4 M in the starting material. Caprylic acid and *n*-butylamine were used as surfactants to modify the surface charge and to control the size, shape and agglomeration of the ZnO particles. NaOH, KOH, HCl, H_2SO_4 and HNO_3 were used as mineralizers in the synthesis experiments. The resultant products were subjected to a systematic characterization using powder XRD, FTIR spectroscopy, SEM, DLS and photoluminescence spectroscopy. Tailoring of the morphology, size and properties could be achieved for these ZnO designer particulates through selective doping, surface modifier and also mineralizer.

Introduction

Zinc oxide (ZnO) is an important wide band gap semiconductor (ΔE =3.37eV at 300 K) with a large exciton energy of 60 meV and thermal energy of 27 meV, and is subject to research as a heterogeneous photocatalyst over the last few years due to its potential to decompose a wide range of organic compounds in water and air at ambient temperature. [1-3]Besides, ZnO possesses a set of unique mechanical, electrical, and optical properties with a combination of high stability, very high melting point with valuable device potential for piezoelectric transducers, gas sensors, optical waveguide, transparent conductive films, varistors, solar cell windows, bulk acoustic wave devices.[4-6] Due to bright UV-luminescence, ZnO is a perspective material for manufacture of UV-light emitting diodes, UV-lasers operating at room temperature and display devices. Moreover, ZnO quantum dots with very low toxicity, high photo stability, biofriendly and biodegradable have been demonstrated. [7-10] Hence, ZnO can be used as a possible replacement for conventional tags and toxic quantum dots like CdTe, CdSe, etc. for biomedical applications. [7-10] In recent years, *in situ* shape and size control of materials have become an important part of materials processing.

Several preparative methods covering both physical and chemical methods have been adopted to synthesize ZnO both as bulk to nanosize particles, films and coatings, etc. However, the physical methods like vapour phase deposition insist upon the extreme operating conditions, which become cumbersome for routine and large scale synthesis. In contrary, the chemical methods like sol-gel, chemical bath, electrochemistry and novel solution routes like hydrothermal, solvothermal and supercritical hydrothermal processes have several advantages owing to the homogeneous or heterogeneous chemical reaction in a closed system through a highly controlled diffusion leading to the formation of polyscale designer particulates with desired morphology and size. [11-13] Several approaches have been adopted by various researchers to control the shape and size and in turn the properties of materials. Amongst them selective doping, precursors used, surfactants, synthesis method, etc. are important ones. In case of ZnO, selective doping is being extensively adopted in order to modify its electronic structure and other physico-chemical properties. The structure of ZnO shows hexagonal symmetry group $P6_3mc$ making possible the lodging of a wide range of atoms, diffusion of the atoms by crystalline lattice or formation of even the respective solid solutions.[14-15] Similarly, surfactants are used largely to control the size, shape and agglomeration of the resultant products. Surfactants also help in modifying the surface charge of crystals and particles, such that, the material becomes either hydrophobic or hydrophilic. Also metal oxides supported with various other oxides for enhanced catalytic applications can be fabricated.[16-17] Here the authors use the term polyscale designer particulates, because of size variation from micron size to nanosize of ZnO particles.[18] In the present work, authors report the hydrothermal synthesis of selectively doped ZnO polyscale designer particulates. The ZnO molarity was varied from 1M - 4M. Metal doping was done with a variety of metals both large and small ion size like Mo, W, Cr, Mn, Fe, Sn, Ag, In, Nd, Cd, etc. with and without surface modifier. The doping of metals is expected to alter the electronic state through the creation of oxygen deficiencies and non-stoichiometry, which in turn varies the photocatalytic properties. Further, doping can alter the morphology of particles, agglomeration, dispersion, and also the size of ZnO particles. Hence the present authors have discussed the hydrothermal synthesis, metal doping, surface modification, and a systematic characterization of ZnO polyscale designer particulates.

Experimental

In the hydrothermal preparation of selectively doped ZnO particles with the size ranging from ultrafine particles to nanoparticles, experiments were carried out using General Purpose autoclaves made up of SS316 (Fig. 1) designed and fabricated at the University of Mysore. India. The autoclaves were provided with Teflon liners (30 ml capacity). The chemical reagents used in the synthesis of selectively doped ZnO polyscale designer particulates are listed in Table 1. A desired amount of zinc oxide with a required molarity was taken as a starting material and a respective dopant was added into it in a required percentage of 1 - 5wt %. A mineralizer of either acidic or basic nature with a definite concentration of 1N - 1.5N was added to the precursors. For experiments in the presence of a surface modifier, the required amount of *n*-butylamine or caprylic acid was added into the above mentioned mixture and stirred vigorously for about 10 min. The final mixture was then transferred into Teflon liner, which was later placed inside the autoclave. The initial *pH* was recorded for this precursor. The pressure inside the autoclave was maintained through percentage fill of precursors in the Teflon liners. The autoclave assembly was placed inside the furnace with a temperature programmer. The experimental temperature was varied from 150 - 250^{o}C depending upon precursors and surface modifier. The experimental procedure is shown in the flow chart (Fig. 2). The characteristic experimental conditions used in the synthesis of selectively doped ZnO polyscale designer particulates are given in Table 2. The crystallization was carried out using spontaneous nucleation and kinetics of crystallization was controlled by varying the experimental parameters such as solvent concentration, surfactant, *pH*, experimental temperature, duration, dopant metal, ZnO molarity, etc. These experimental parameters play a dominant role in controlling the morphology, size and also properties.

After the hydrothermal treatment, the autoclave was quenched and Teflon liner was taken out. The final *pH* was measured. The resultant product was transferred into a clean beaker and washed with double distilled water. The surplus solution in the resultant product was removed using a syringe and the remnants were centrifuged for 20 minutes at 3000 rpm. The product was recovered and dried in a hot air oven at 50^{o} C for a few hours. The presence of surfactants greatly influences the surface charge and also the size [19-22]. When *n*-butylamine was used, the product was hydrophilic. In contrary, when caprylic acid was used, the resultant product was hydrophobic. The dried particles were subjected to a systematic characterization using powder XRD, FTIR, SEM, DLS, and photoluminescence spectroscopy.

The addition of surface modifiers also helps to inhibit the crystal growth that facilitates the smaller particles size with a narrow particle size distribution. When the *pH* of the reaction medium is highly acidic or highly basic, very small particles along with the large particles are formed leading to a broader size distribution. It seems that because of redissolving of nanoparticles at very high and low *pH*, Ostwald repining occurs. Therefore, in surface modification, *pH* of the medium, isolectric point (IEP) and another important parameter, viz. dissociation constant (*pKa*) of the modifiers are very important. At *pH* below *pKa*, the modifier does not dissociate. Moreover, below *IEP*, the surface of metal oxide nanoparticles is surrounded by positive charges (major) and hydroxylic groups (minor). Under these conditions there is no chemical reaction occurring between the modifier and the metal oxide nanoparticle surface, but it is only through a strong hydrogen bonding the modifier can attach to the nanoparticles surface. In contrary, at higher *pH* than *pKa*, dissociation of modifier takes place and results in chemical reaction between dissociated part of modifier and OH^- from particles surface. Thus, by dehydration reaction modifier attaches to the surface of the particles. By considering the chemical reactions, mass balances, charge balance in the actual system, *pH* and the modifier can be fixed for most of the systems. The other important point to be noted here in these hydrothermal experiments with surfactants is that the initial *pH* and final *pH* do not vary much like in the case of conventional hydrothermal experiments without surface modifiers. These modifiers help to maintain the desired *pH* and the ionic strength of the solvent in the hydrothermal media, and hence they play a very important role during hydrothermal crystallization. With a rise in the molarity of ZnO, the formation of ZnO ceases in spite of maintaining other parameters constant.

Characterization

The selectively doped ZnO polyscale designer particulates were characterized using various analytical techniques. The powder X-ray diffraction (XRD) patterns were recorded using a RIGAKU system (Ultima III series, TSX System and Miniflex XRD, Japan). The scanning range was 10-80^o (2Θ) with scanning speed of 2^o min^{-1} with CuKα, λ=1.542 Å, radiation voltage = 40 KV, Current=40 mA. The Fourier transform infrared (FTIR) spectra were recorded in the range 4000-400 cm^{-1} using JASCO-460 Plus, Japan, at a resolution of 4 cm^{-1}. The sample was

dispersed in KBr in the ratio 100: 1 = KBr: Sample. Scanning electron microscopy (SEM) images were taken using field emission SEM (FESEM, HITACHI, S-4200, Japan). The optical properties were studied using UV-Vis Spectrophotometer (Minispec SI 171, ELICO, India). The particle size of selectively doped ZnO polyscale designer particulates was measured using dynamic light scattering (DLS) method (HORIBA, LB-550, Japan). The unpolarized photoluminescence (PL) was measured at 10K. The photoluminescence signal from excitation with a He-Cd laser (λ = 325 nm, P_{out} = 1-1.6 mW) after dispersion on a 30 cm triple grating monochromator was detected by a CCD camera (Princeton Instruments Inc., USA).

Results and discussion

The products were highly crystallized and the powder XRD analysis reveals wurtzite structure with all peaks matching with the standard JCPDS file (PDF File No.36-1451), space group $P6_3mc$ of dihexagonal pyramidal class. The cell parameters of doped ZnO were calculated using check cell software. [23] Table 3 gives the cell parameters of the selectively doped ZnO polyscale designer particulates. Fig. 3*a-h* show characteristic XRD patterns for doped ZnO polyscale designer particulates. The cell parameters change slightly with respect to the type of dopant used and the amount of dopant used is constant (1 wt%) in all cases. Also there is no regularity in the increase or decrease in the lengths of the *a* or *c* axes and also the volume of the selectively doped ZnO. It is interesting to note that the XRD data does not vary for doped ZnO polyscale designer particulates obtained in the presence or absence of the surfactant. However, it is interesting to observe variation in the phase homogeneity with respect to the concentration and type of the dopant metal. Also it was observed that not all the dopant metals used in the present experimental work enter into the ZnO structure homogeneously irrespective of the concentration variation from 1 to 5 wt% in some cases even 10 wt%. When Sn and Ag were used as dopants in small quantity like 1 wt%, there is a homogeneous structure of ZnO and the powder XRD patterns do not vary from the standard ones (Fig.3a,b). Even the optical quality of these polyscale designer particulates is very high as observed from the PL spectra. In fact, the optical quality is enhanced in these cases. However, when the concentration of these metals is increased, a compositional inhomogeneity was observed both from XRD, SEM and PL spectra. These dopants form their chlorides what is clearly observed from the XRD patterns and SEM images. Therefore, 1 wt% Ag or Sn doping enhances both optical quality (as observed from PL spectra)

and photocatalytic property of ZnO significantly (as observed from the organics degradation studies discussed later). In contrary to this, the dopants like Cd, Mo, W, and Nd clearly indicate a kind of phase inhomogeneity in the product, and the XRD patterns indicate a kind of mixed phases such as ZnO, with unreacted reagents / sources of dopants, or some hydroxides, and chlorides of dopant metals, even when these dopants are used in small concentration **(Fig. 3c-g).** The FTIR spectroscopy data reveals that as the dopant metal and its percent concentration are changed, there is a shift of peak positions in the ZnO band region (Fig. 4*a-c*). As evident from Fig. 4, it is observed that peaks occurring in the region 400-500 cm^{-1} are due to the stretching mode of the Zn-O bond. In contrast the characteristic absorption band of ZnO shifts from 438-453 cm^{-1} for the doped ZnO polyscale designer particulates. The absorption band in the region 3000 – 3800 cm^{-1} corresponds to OH^- mode. The stretching bands in the region 500-1020 cm^{-1} correspond to O - dopant metal - O bond as observed from Figure.4. The band in the region 1003 - 1012 cm^{-1} is due to the symmetrical mode of W- 0 stretching mode of the tungsten oxide complex. Similarly, the Cd – O bond shows the highest stretching frequency at 993 cm^{-1} and Mo shows the stretching frequency at 817 cm^{-1}. Further from Fig. 4, it is observed that the bands in the region 1633 cm^{-1}, 1500 cm^{-1}, 1352 cm^{-1}, 1352 cm^{-1}, and 698 cm^{-1} represent δ(HOH), δ(OH), and γ(OH) mode .[24,25] **[28,29]**

SEM images were recorded for the representative samples of selectively doped ZnO polyscale designer particulates in order to know the influence of dopant metal on the morphology and also the particle size. In the present study of crystal morphology of doped ZnO varies from several micron size to nanosize particulates. The observations made from the SEM study well correlate with the powder XRD data. Fig. 5*a-j* show the representative morphologies obtained for selectively doped ZnO polyscale designer particulates. The morphology on the whole is represented as hexagonal plates, rectangular, short/long hexagonal prisms, fibrous, irregular, etc. On the whole the selectively doped ZnO polyscale designer particulates show well developed morphology, particularly when 1 wt% ZnO was used in the starting materials. Also particles are less agglomerated, because of the presence of surfactant. When no surfactant was added in the starting precursors, the products appeared more agglomerated and this was also observed in experiments with higher molarity of ZnO in the starting materials. The surfactants are the fatty acids and become miscible with aqueous solutions at higher temperature or supercritical

temperature and contribute to the formation of ZnO polyscale designer particulates with desired size and shape. A combination of inorganic materials at the nano-size with the organic molecules could solve several problems encountered in the application of nanoparticles, and it led to the emergence of the *in situ* surface modification of nanoparticles with a great variety of organic surface modifiers, which bring in a perfect dispersion of the nanoparticles in solvents or in polymers. In order to resolve the problem of particle aggregation, to achieve the perfect control over the size and morphology of the particles, and to obtain a desired surface property to the nanoparticles, a new processing strategy has been proposed .[26-29] **[19-22]** This strategy is highly effective for the synthesis of organic-ligand assisted hydrothermal technology. The method yields perfect hybrid organic-inorganic nanoparticles with very high dispersibility, and a precise control over the size and shape of the nanoparticles. The organic components are introduced into the system during the hydrothermal synthesis and *in situ* surface modification is obtained with an ultra-thin layer of organics surrounding the inorganic unlike the case of silane coupling on the metal oxides. The organic ligands and supercritical water form a homogeneous phase and it is known that under these conditions water molecules themselves work as acid or base catalyst for various organic reactions. Depending upon the applications of nanoparticles, one can select suitable functional groups to introduce hydrophobicity or hydrophilicity property to the surface of the modified nanoparticles. In aqueous systems, metal oxide particles are hydrated and M-OH groups cover completely their surface and the surface is neutral. The M-OH sites on the surface of particles can react with H^+ or OH^- ions from dissolved acids or bases, and positive ($M\text{-}OH^{2+}$) or negative ($M\text{-}O^-$) charges develop on the surface, and type of the reaction depends on *pH* of the solution. In the absence of specific adsorption of ions, amphoteric metal oxides have a characteristic *pH*, the *pH* of the point of zero charge (PZC), where the net surface charge is zero, i.e. the positive and negative sites are in equal amount (isoelectric point, *iep).* At pH lower than *iep*, the pure metal oxide surface is positively charged, while it has negative charge above it. [30-32] **[23-25]** Normally the modifiers attach onto the surface of the nanoparticles either by physisorption or chemisorptions through a strong hydrogen bond. If we consider R-COOH as modifier reagents in a highly acidic *pH* of the reaction medium, the dissociation of modifier does not occur and the conjugation is due to the strong hydrogen bonding between hydroxylic groups on the surface of nanoparticles and functional groups of modifier .[33] **[26]** If the pH of the reaction medium is in the range of modifier dissociation, another type of interaction between the modifier and the metal

oxide surfaces is expected. [34] [27] Similar chemical bonding is expected even for amines or alcohol or aldehyde as the organic ligands in the system.

The crystal size varies from 25 μm (as in the case of Mo doping Fig.5g) – 10 nm. Hence the authors have used the term polyscale designer particulates in the present work, and this SEM based size data matches well with the DLS data. Here it is appropriate to mention that the surfactants contribute greatly on the size of the ZnO designer particulates, and the size is reduced when the surfactant is used. When the molarity of the ZnO in the raw material is increased to 4M, the ZnO particulates tend to loose their facets and become fibrous and porous (Fig 5 *j*). On the whole as observed from SEM images that lower concentration of dopants result in the formation of particles with well developed morphology for ZnO, and the same in the presence of surfactant result in the formation of small size designer particulates with lower aspect ratio. When the dopant concentration is high irrespective of the presence or absence of surfactants, it results in the formation of highly irregular, acicular, fibrous, particulates and often as mixed phases.

Dynamic light scattering study for the evaluation of the size distribution profile was carried out for the doped ZnO ultra fine to nanosize designer particulates. The histograms showing the distribution of the population of particles with respect to the particle size for the characteristic samples of selectively doped ZnO designer particulates are given in Fig. 6*a-c*.

Photoluminescence (PL) spectroscopy is a nondestructive and highly sensitive method of probing the optical quality of materials. The PL emission originates from the surface-near volume of a material, and is sensitive to surface defects and chemical homogeneity of the material, especially when the dopant is added to the host material.

In the present work PL studies of ZnO polyscale designer particulates selectively doped with Cd, Mo, W, Nd, Sn, Ag in different concentrations and with 1M ZnO in the nutrient have been carried out to understand the change in electronic and also crystal chemical properties of ZnO with respect to the dopant metal and its concentration. Fig. 7*a-f* show the results from PL measurements the near band edge emission in the range 2.8 – 3.5 eV upon laser excitation at λ_{em} = 325 nm (3.815 EV). Generally, for high-quality ZnO we do find the donor bound exciton (D^0X) related peak emission around 3.36 eV (depending on the donor ion) and different states of

free A-excitons (FX_A) peaking around 3.377 eV and 3.42 eV, respectively. On the low energy side is the two electron satellite (TES; 2s and 2p state) transitions of the neutral donor bound exciton recombination peaking between 3.31 and 3.33 eV.[35] bm The longitudinal phonon replicas from D^0X , D^0X_{nLO} with n = 1 to 4 are clearly obtained at 3.2907, 3.2178, 3.1462, and 3.0734 eV, respectively.

The doping of ZnO with Cd, Mo, W, and Nd show a stronger TES than D^oX peak in terms of absolute intensity (Fig.7a-d). In contrary, Ag and Sn are quite interesting as dopants and the TES peaks are not stronger than D^oX peaks (Fig.7e,f). Further observed from the PL spectra, lower concentration of 1 to 3 wt % Cd is acceptable within the ZnO lattice, and with 10 wt % Cd, D^oX is very small, pointing to poor optical quality as a result of increased defect concentration in the crystal lattice. Free exciton emission for 1 and 3 wt % doping is clearly visible, but absent for 10 wt% doping. Clearly, a higher concentration of Cd is worsening the optical quality of ZnO. The same holds true for the case of Mo doping, where lower concentration of Mo leads to obtain optically good quality ZnO, and higher concentration of Mo leads to the structural distortion and it contributes to the worsening of the photocatalytic properties also. Figure 8a shows the photocatalytic efficiency under the exposure of ultraviolet light for Mo doped ZnO in the treatment of textile effluents, which are rich in toxic organic dyes. Structurally both Cd and Mo have similar effect on ZnO. Likewise, surplus doping with W and Nd worsens the quality of ZnO rather behaving like metals due to the Burstein-Moss shift.[36] *n*-type semiconductor properties will be obtained. In contrary, the 1 wt % doping of Sn gives highest emission peak at 3.36 eV, and 5 wt% and 10 wt% doping with Sn do not alter this emission, but the intensity is reduced. The free exciton energy is clearly visible pointing to higher optical quality. To conclude, a lower concentration of Sn is getting into the structure independent of its initial concentration. Doping of ZnO with Ag has given very interesting results which could be well correlated with the powder X-ray diffraction and SEM data. Surplus Ag doping like 10 wt% lead to the formation of heterogeneous structures and we can even observe separate formation of $AgCl_3$ phase attaching onto the surface of ZnO. But lower concentrations of Ag doping leads to the synthesis of ZnO with higher optical quality and the emission peaks correspond to the 3.36 eV due to D^oX. However, with the variation in the concentration of Ag, the intensity of TES peaks does not vary; whereas the intensity of emission peaks at 3.36 eV vary significantly upon 10wt% doping. Thus both smaller concentrations of Ag and Sn as dopants enhance the optical quality of ZnO and in

turn the photocatalytic properties also enhanced significantly. Figure 8b shows the photocatalytic efficiency of Sn doped ZnO in the treatment of pharmaceutical effluent under the exposure of sun light. Therefore, selective doping of ZnO with an appropriate dopant in a specific concentration can lead to the formation of higher optical grade ZnO polyscale designer particulates. The hydrothermally prepared selectively doped ZnO polyscale designer particulates show far emission to near visible light emission between 369.4 - 401 nm with an improvement in the photoluminescence property, *i.e*. the photoluminescence emission wavelength shifts from UV region to visible region, when compared with commercial and synthetic pure ZnO sample.[35-38] [31-34] From the above observations, it can be concluded that by the doping with the above metal ions into ZnO host lattice the bandgap of the photocatalytic compounds can be altered and that in turn will affect the photocatalytic properties.

Conclusion

Hydrothermal synthesis of ZnO under mild *PT* conditions in the presence of a variety of metal ions and an appropriate surface modifier has led to the formation of tailored morphology, size and properties for the resultant products. Depending upon the type of dopant metal and its concentration, the morphology of the ZnO varied from hexagonal plates, hexagonal prisms, rectangular plates, sub-rounded particles, fibres, needles, etc. Also when the molarity of the ZnO in the starting material was increased to 4M, the product becomes more fibrous and porous. Beyond this molarity, the crystallization of ZnO ceases. The size of the ZnO particles varied from 25 μm – 10 nm depending upon the experimental parameters. All the resultant products had high degree of crystallinity. The use of surfactant assisted in reducing the size and agglomeration of the designer particulates. The concentration of the surfactant is also an important parameter in order to bring down the size and shape of the particles. Caprylic acid resulted in the synthesis of hydrophobic ZnO particles, where as *n*-butylamine resulted in the synthesis of hydrophilic ZnO particles. XRD data revealed homogeneous product. FTIR spectroscopy data indicated the presence of these surface modifiers and also the appearance of the dopant metal – oxygen bands. SEM images show well developed morphology for the ZnO particles. The crystals are on the whole well faceted showing large hexagonal plates, rectangular plates, prismatic rods, etc. Photoluminescence spectroscopy studies indicated the change in the bandgap and the emission shifting from UV region to visible region, when compared with commercial and synthetic pure

ZnO sample. This would be highly useful in the photocatalytic application and also in the fabrication of UV-sensor devices.

References

1. M.R. Hoffman, S. Martin, W. Choi, D.W. Bahnmann, Chem. Rev. 1995, **95,** 69-72.
2. J. Peral, X. Domenech, D.F. Ollis, Chem. Tech. Biotech. 70 (1997) 117.
3. A.L. Linsebigler, G. Lu, J.J.T. Yates, Chem. Rev., 95 (1995) 735.
4. D. Ehrentraut, H. Sato, Y. Kagamitani, H. Sato, A. Yoshikawa and T. Fukuda, *Prog. Cryst. Growth Charact. Mater.*, 2006, **52**, 280-335.
5. T.L. Yang, D.H. Zhang, J. Ma, H.L. Ma, Y. Chen, Thin Solid Films 326 (1998) 60.
6. P. Verardi, N. Nastase, C. Gherasin, C. Ghica, M. Dinescu, R. Dinu, C. Flueraro, J. Crystal Growth 197 (1999) 523-.
7. D.P. Liu, G.D. Li, Y. Su, J.S. Chen, Angew. Chem., 118 (2006) 7530-7533.
8. D. Vollath, I. Lamparth, D.V. Szabo, J. Nanoparticle Res., 6 (2004) 181-191.
9. Y.L. Wu, A.I.Y. Tok, F.Y.C. Boey, X.t. Zeng, X.H. Zhang, Appl. Surface Sci., 253 (2007) 5473-5479.
10. J. Zhou, N. Xu, Z.L. Wang, Adv. Mater., 18 (2006) 2432-2435.
11. L. Yuzhen, G. Lin, X Huibin, D. Lu, Y. Chunlei, W. Jiannong, G Weikun, Y Shihe and W Ziyu, (2006). *J. Appl. Phys.*, 99, 114302.
12. K. Byrappa and M. Yoshimura, *Handbook of Hydrothermal Technology*, Noyes Publications, New Jersey (2001).
13. M. Yoshimura and K. Byrappa, J. Mater. Sci., **43** (2008) 2085.
14. B.S. Barros, R. Barbosa, N.R. dos Santos, T.S. Barros and M.A. Souza, Inorg. Mater., 42 (2006) 1348-1351.
15. I. Ender Suvaci and Ozgur Ozer, J. Eur. Ceram. Soc., 25 (2005) 1663-1673.
16. K.Y.S. Ng, E. Gulari, J. Catal. 92 (1985) 340.
17. T. Machei, M. Remy, P. Ruiz, B. Delmon, J. Chem. Soc. Faraday Trans. 86 (1990) 723.
18. K. Byrappa, In: Springer Handbook of Crystal Growth, G. Dhanaraj, K. Byrappa, V. Prasad and M. Dudley (Eds.), Springer-Verlag Publishers, Germany (2010) pp. 599-653.
19. K. Byrappa, S. Ohara and T. Adschiri, Adv. Drug Deliv. Rev., 60(3) (2008) 299-327.
20. J. Zhang, S. Ohara, M. Umetsu, T. Naka, Y. Hatakeyama and T. Adschiri, Adv. Mater. 19(2)

(2007) 203-206.

21. T. Mousavand, S. Ohara, M. Umetsu, J. Zhang, S. Takami, T. Naka and T. Adschiri, J. Supercritical Fluids 40(3) (2007) 397-401.
22. T. Adschiri and K. Byrappa, In: *Nanohybridization of Organic-Inorganic Materials*, Eds: Atsushi Muramatsu, Publishers: Springer-Verlag, Germany. Pp.217-250.
23. Z. Sun, F. Su, W. Forsling and P.J. Samskog, J. Colloid Interface Sci., 197(1) (1998) 151-159.
24. E. Tombacz, C. Csanaky and E. Illes, Colloid Polym. Sci., 279(5) (200) 484-492.
25. E. Illes and E. Tombacz, J. Colloid Interface Sci., 295 (2006) 115-123.
26. A.S. Piers and C.H. Rochester, J. Colloid Interface Sci., 174(1) (1995) 97-103.
27. S. Liufu, H. Xiao and Y. Li, J. Colloid Interface Sci., 281(1) (2005) 155-163.
28. K. Nakamoto, *Infrared Spectra of Inorganic and Co-Ordination Compounds*, M. Mir, Moscow (1966).
29. I.P. Donald, M.L. Gary and S.K. George, In: *Introduction to Spectroscopy*, 3rd Edition, Thomson Learning, USA, (2001) pp. 13-101.
30. T.H. Gfroerer, Encyclopedia of Analytical Chemistry, John Wiley & Sons Ltd., USA (2000) Pp.9209-9231.
31. C.C. Hsu and N.L. Wu, J. Photochem. Photobiol. A: Chem. 172 (2005) 269–274.
32. H. Shibata, M. Watanabe , M. Sakai, K. Oka, P. Fons, K. Iwata, A. Yamada, K. Matsubara, K. Sakurai, H. Tampo, K. Nakahara and S. Niki, Physica Status Solidi (C) 1 (2003) 872.
33. A. K. Mishra, S. K. Chaudhuri, S. Mukherjee, A. Priyam, A. Saha, D. Das, J. Appl. Phys. 1022007) 103514.
34. M. Yoneta, K. Yoshino, M. Ohishi, M. Honda and H. Saito, Physica Status Solidi [C], 3 (4), (2006) pp. 1185-1188.

35 . Meyer, B.K.; Alves, H.; Hofmann, D.M.; Kriegseis, W.; Forster, D.; Bertram, F.; Christen, J.; Hoffmann, A.; Straßburg, M.; Dworzak, M.; Haboeck, U.; Rodina, A.V. *Phys. Status Solidi B* **2004**, *241*, 231.

36 **bu**. E. Burstein, *Phys. Rev.* 1954, **93**, 632; T.S. Moss *Proc. Phys. Soc. (London)* 1954, **B76**, 775

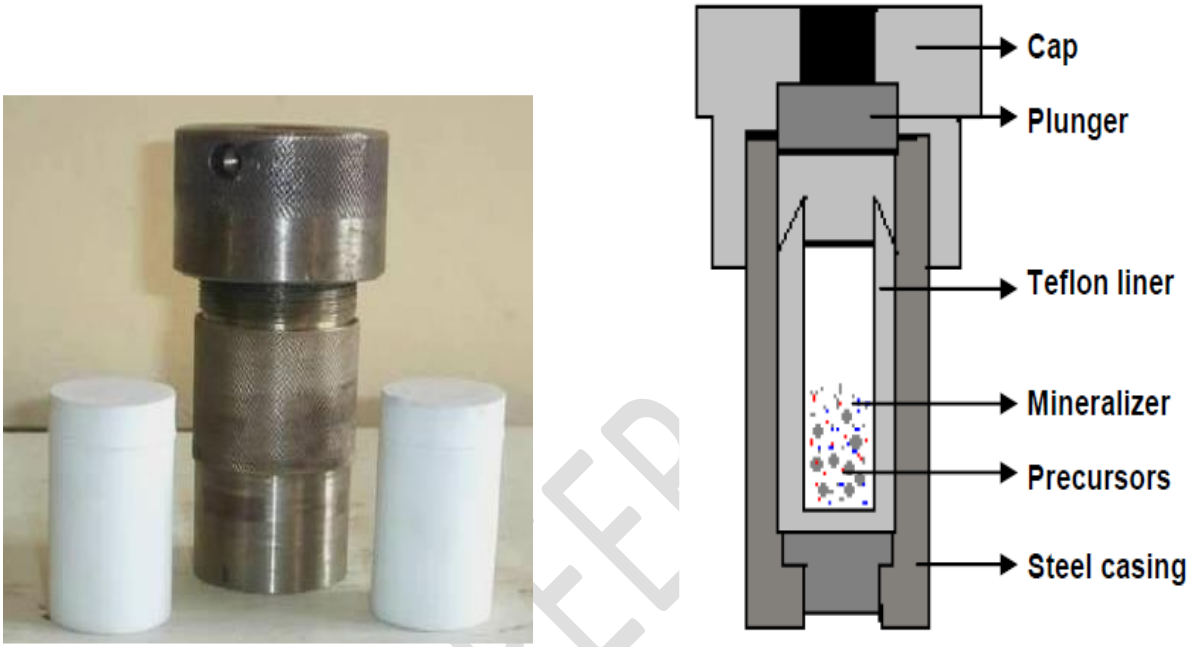

Fig. 1. Hydrothermal autoclave, Teflon liner, and schematic diagram of the cross section of the autoclave used in the synthesis of selectively doped ZnO polyscale designer particulates.

Precursors: L.R. grade ZnO, ZnCl, and metal oxides/chlorides/nitrates for doping – Cr, Mn, Fe, Cd, Sn, Ag, Nd, In, Mo, W, etc.

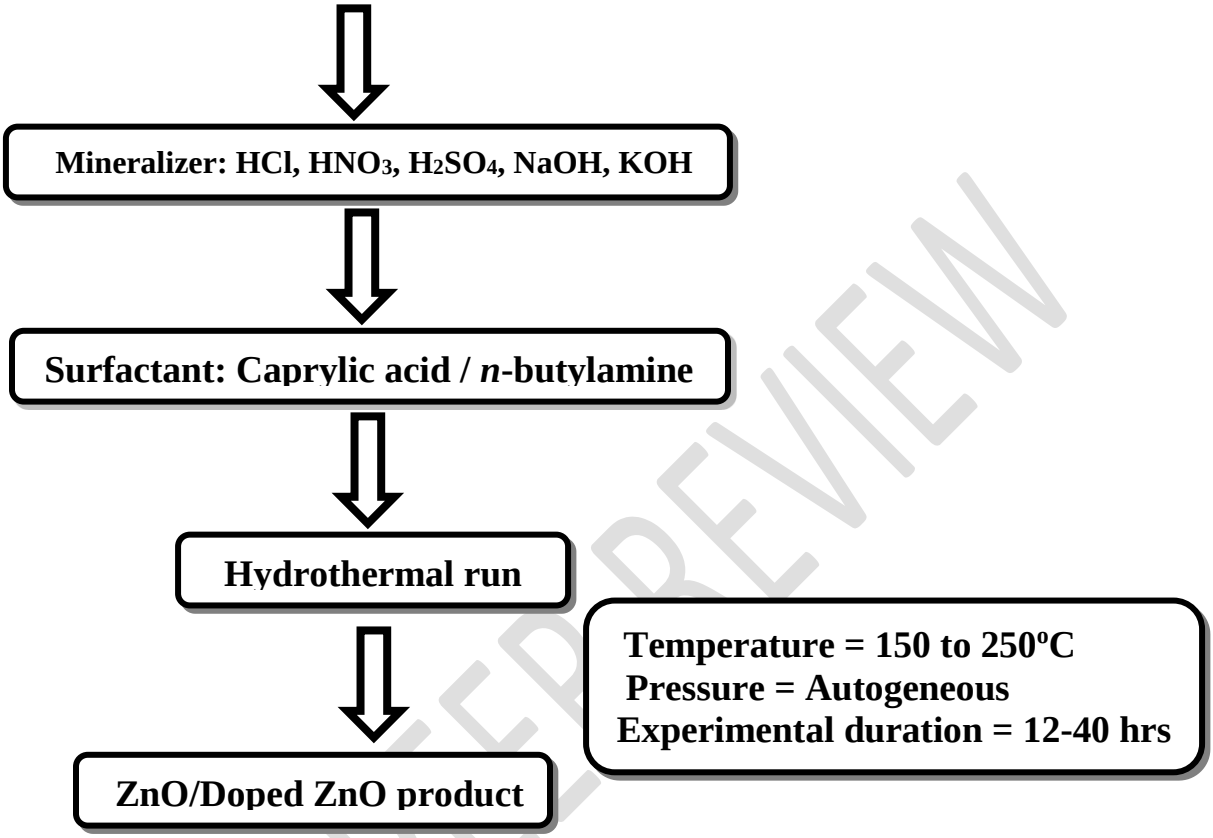

Fig. 2. Flow Chart of the hydrothermal reaction for ZnO synthesis

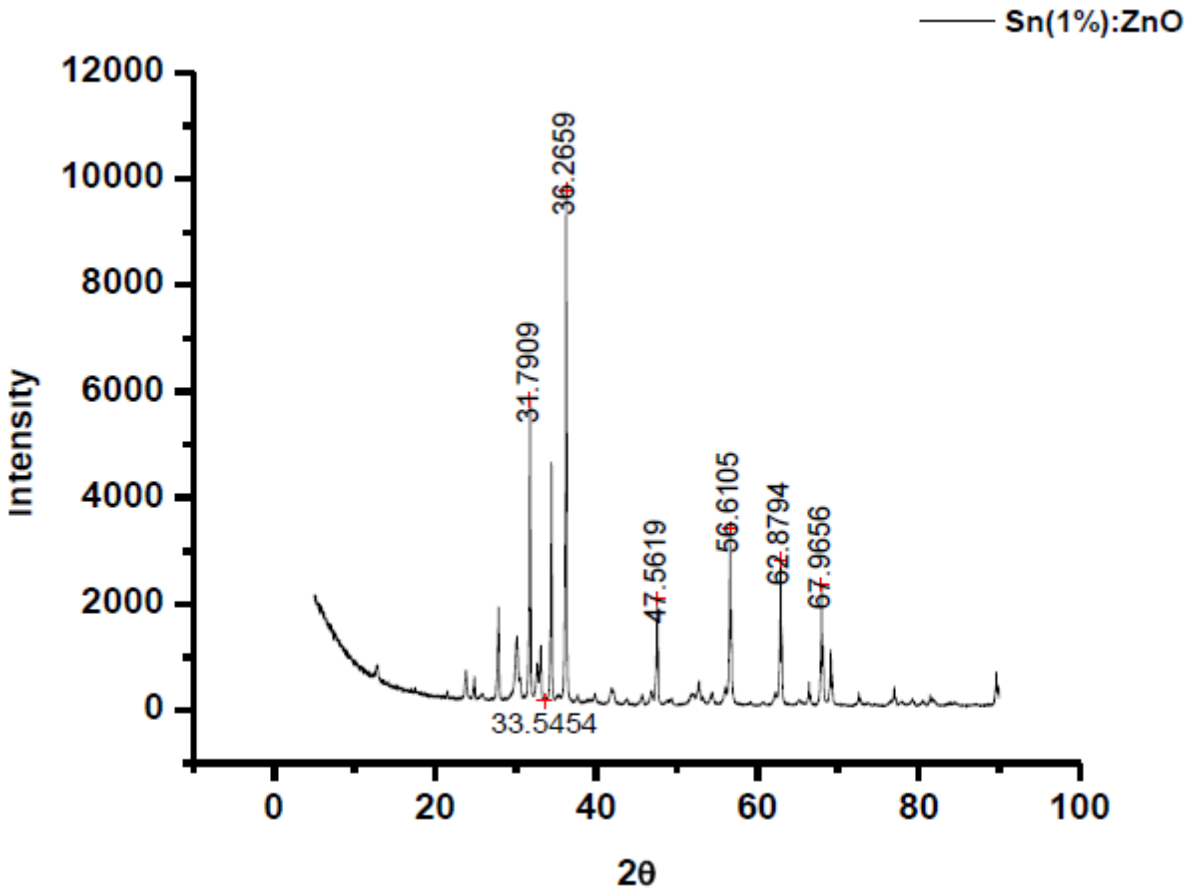

Fig. 3a. X-ray diffraction pattern of Sn doped ZnO

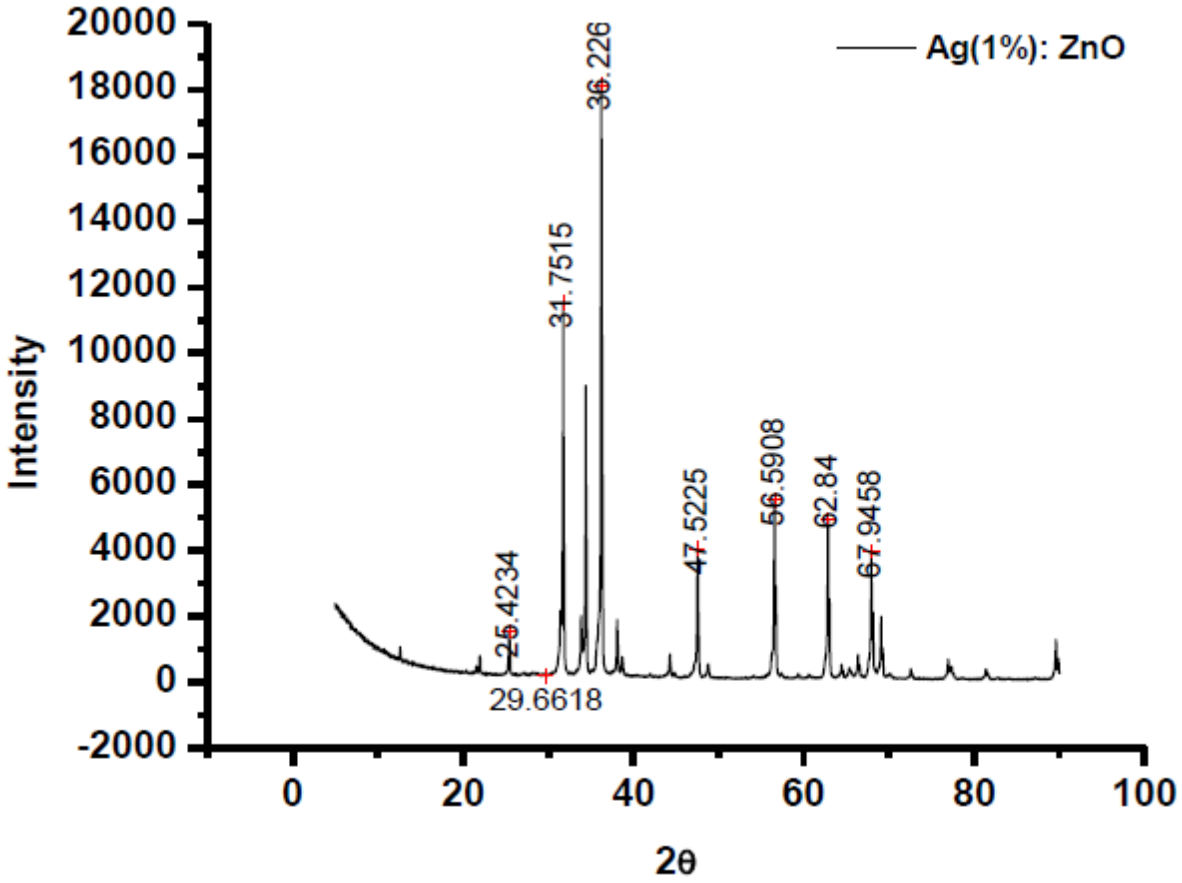

Fig. 3b: X-ray diffraction pattern of Ag doped ZnO

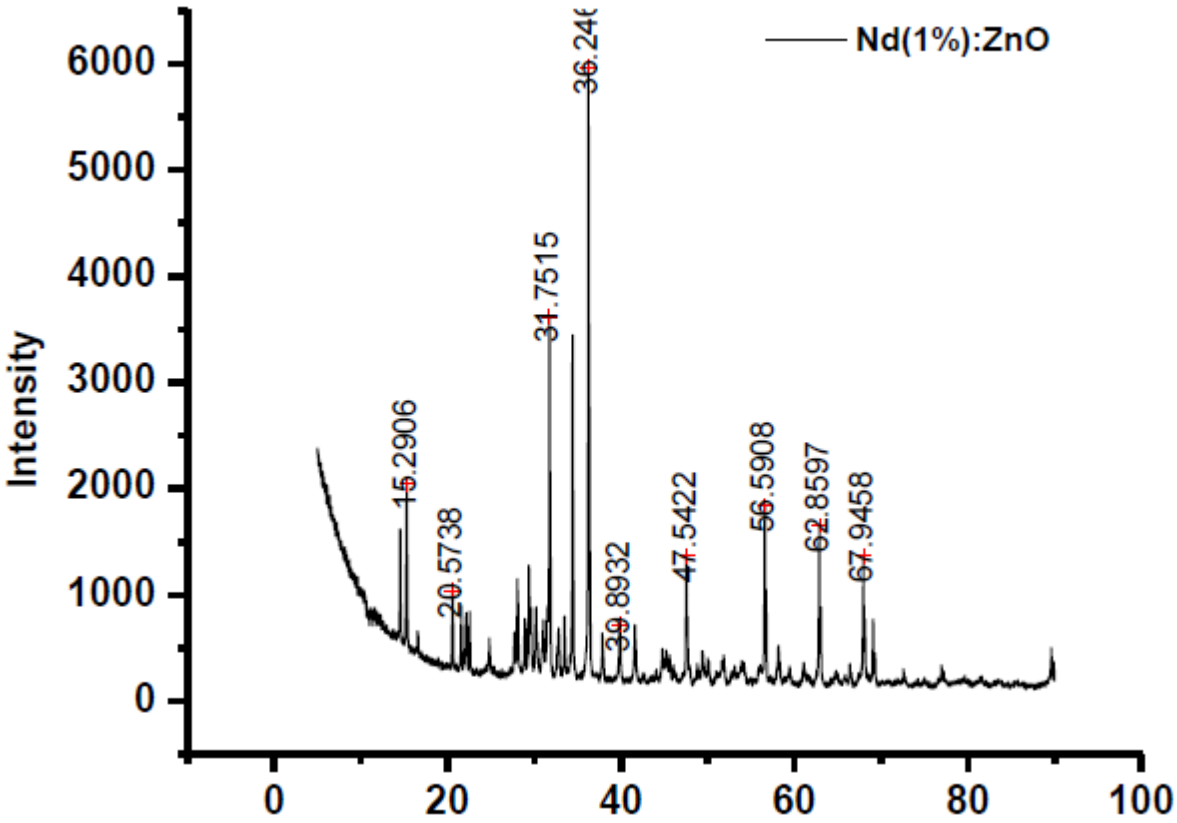

Fig.3c. X-ray diffraction pattern of Nd doped ZnO

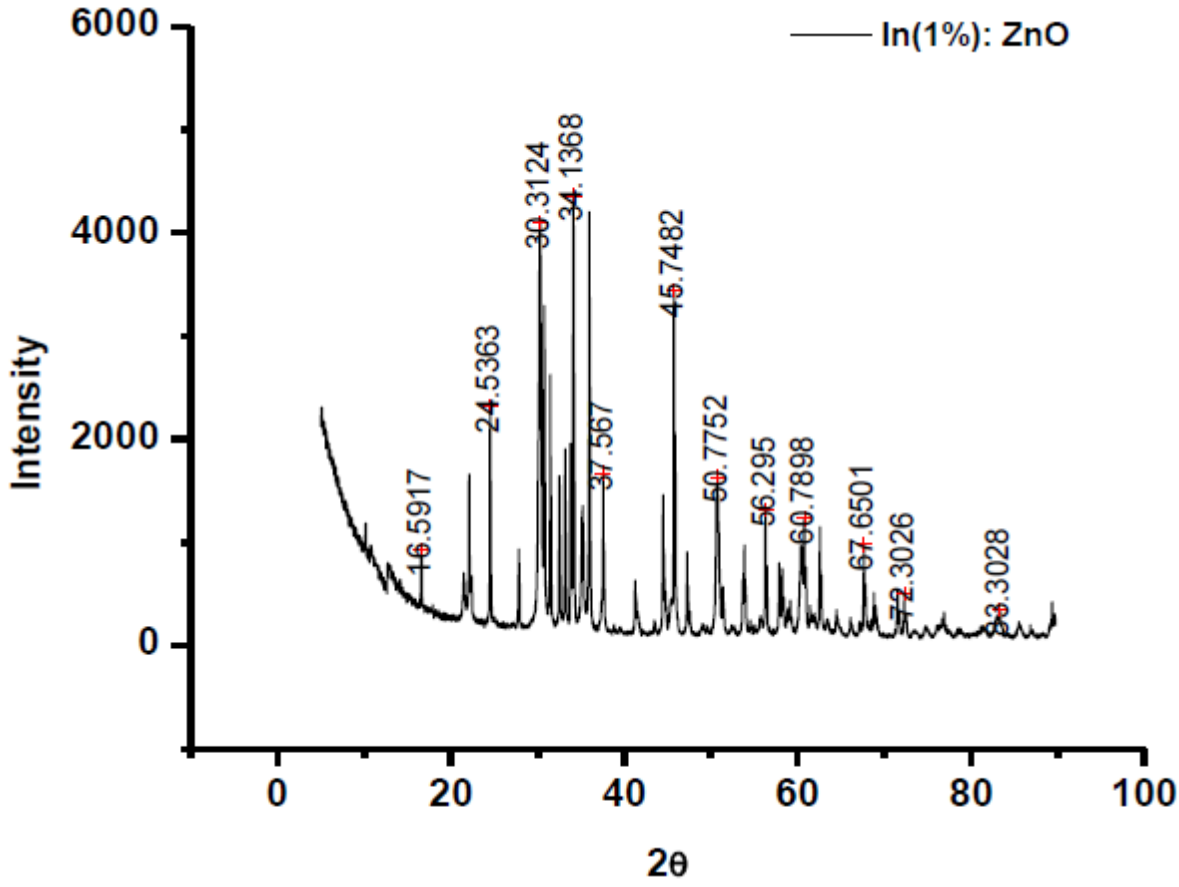

Fig. 3d. X-ray diffraction pattern of In doped ZnO

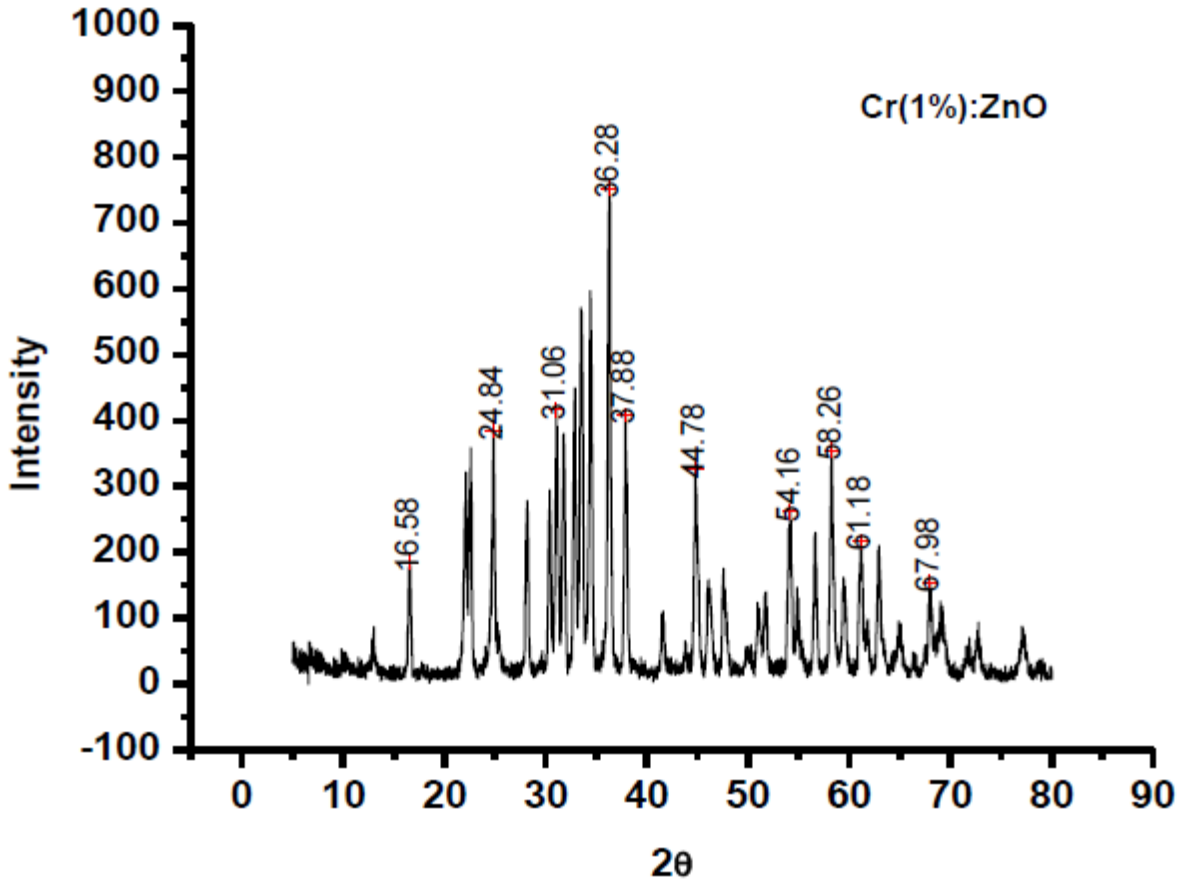

Fig. 3e: X-ray diffraction pattern of Cr doped ZnO

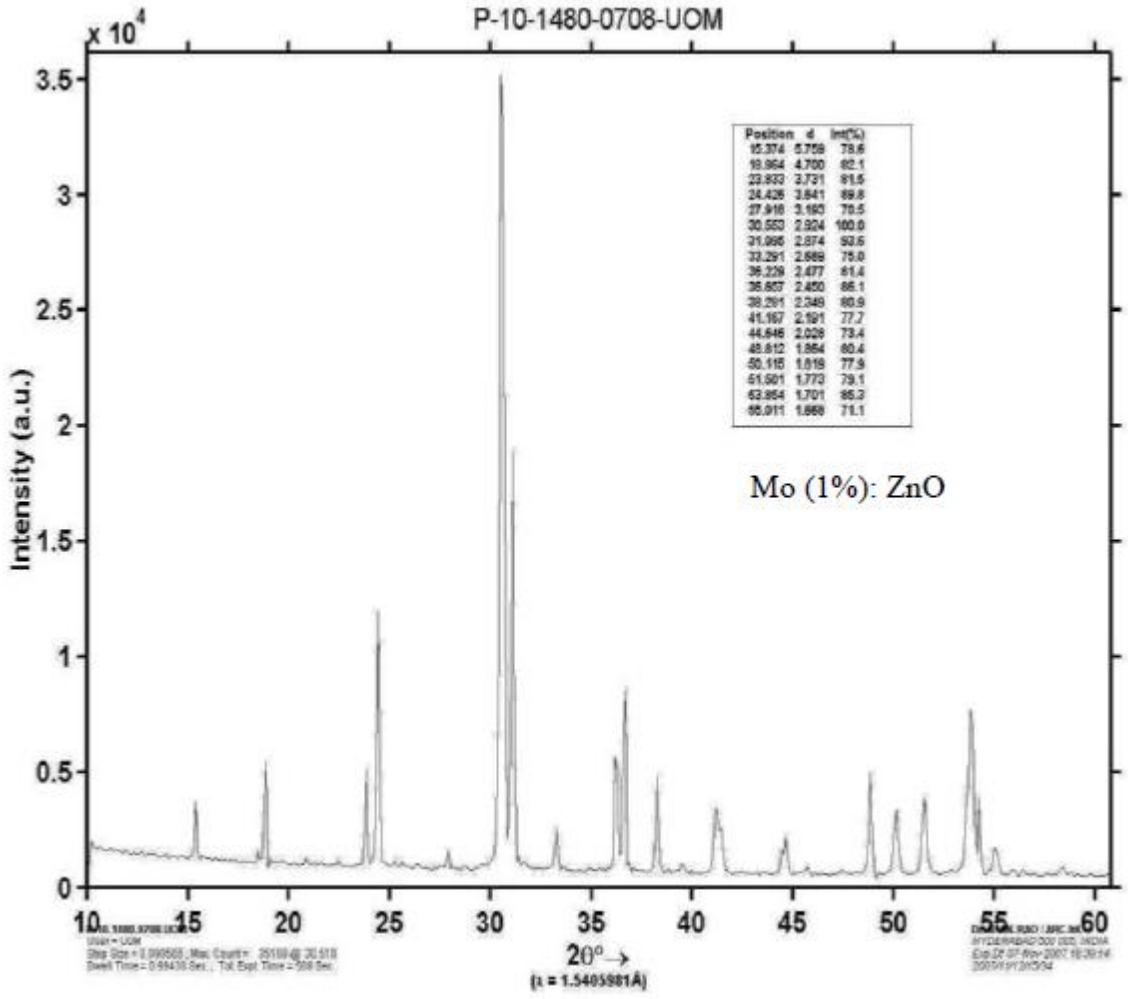

Fig. 3f: X-ray diffraction pattern of Mo doped ZnO

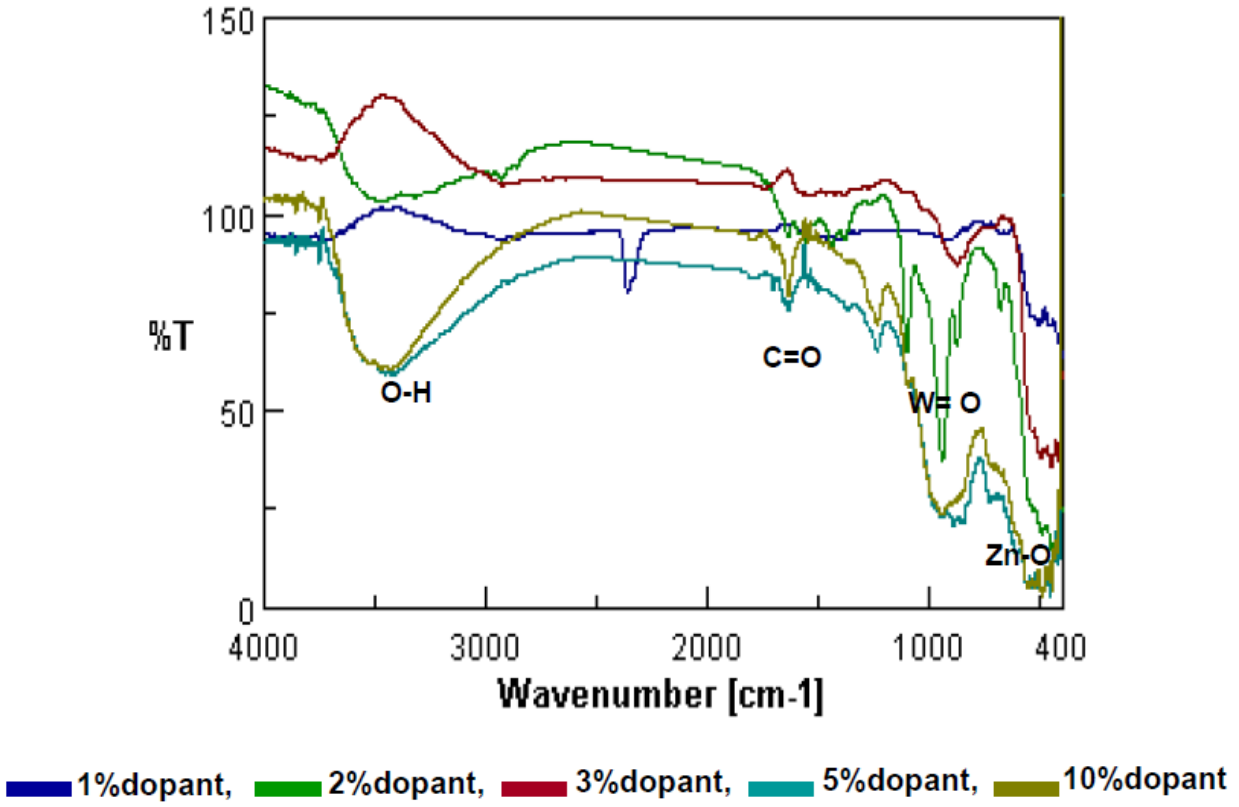

Fig. 4a. FTIR spectra of W^{6+}doped ZnO

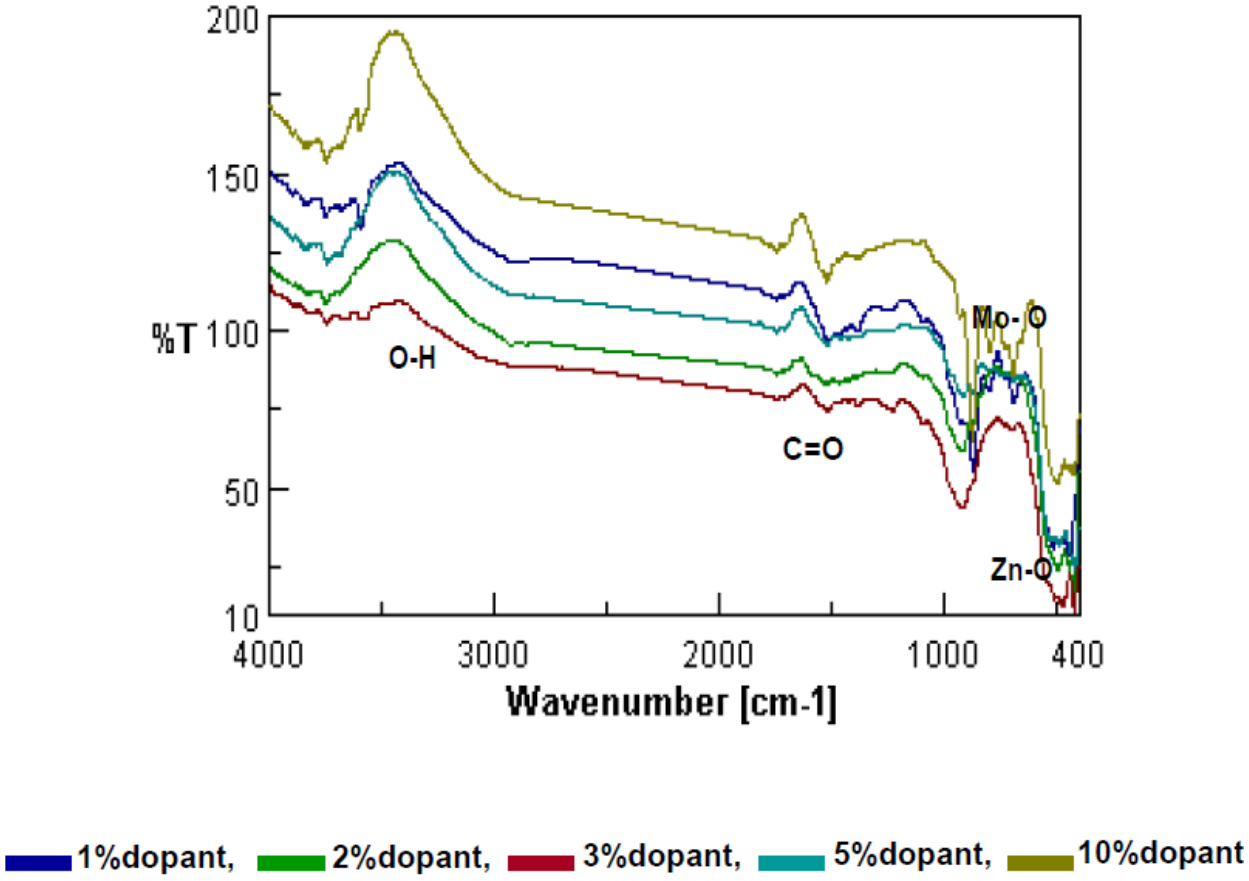

Fig. 4b. FTIR spectra of Mo doped ZnO

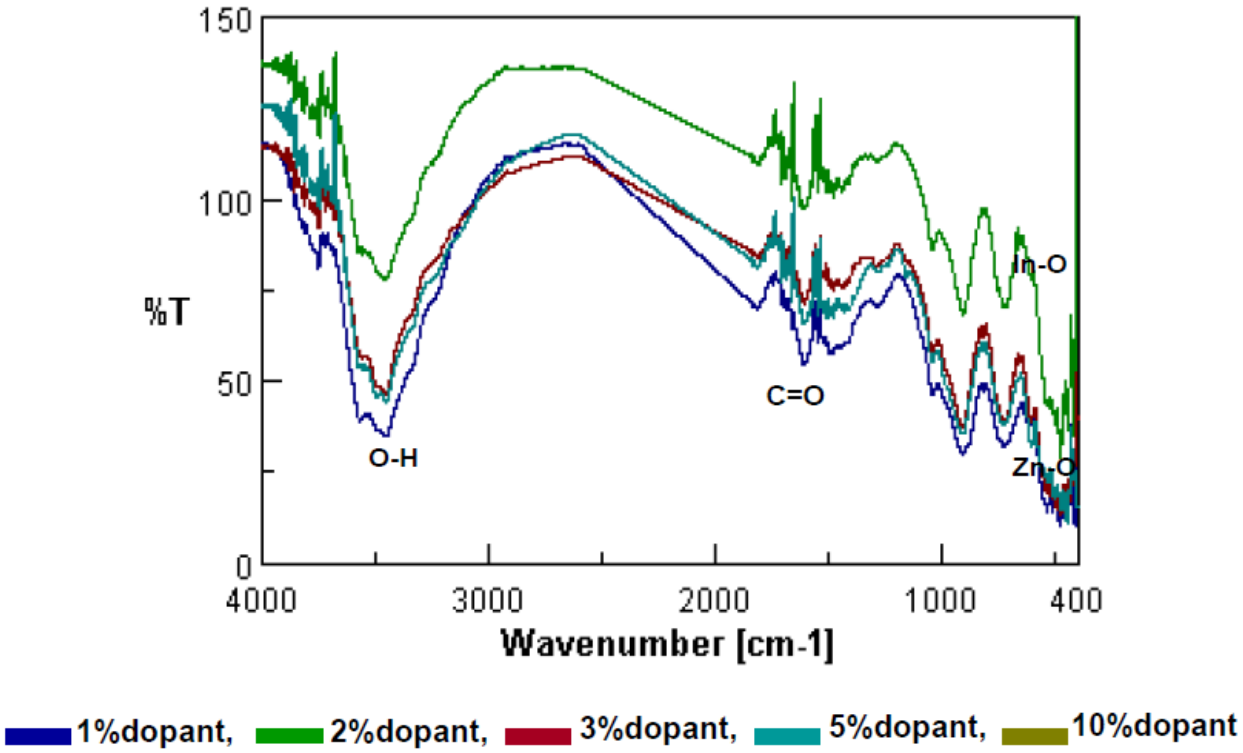

Fig. 4c. FTIR spectra of In doped ZnO.

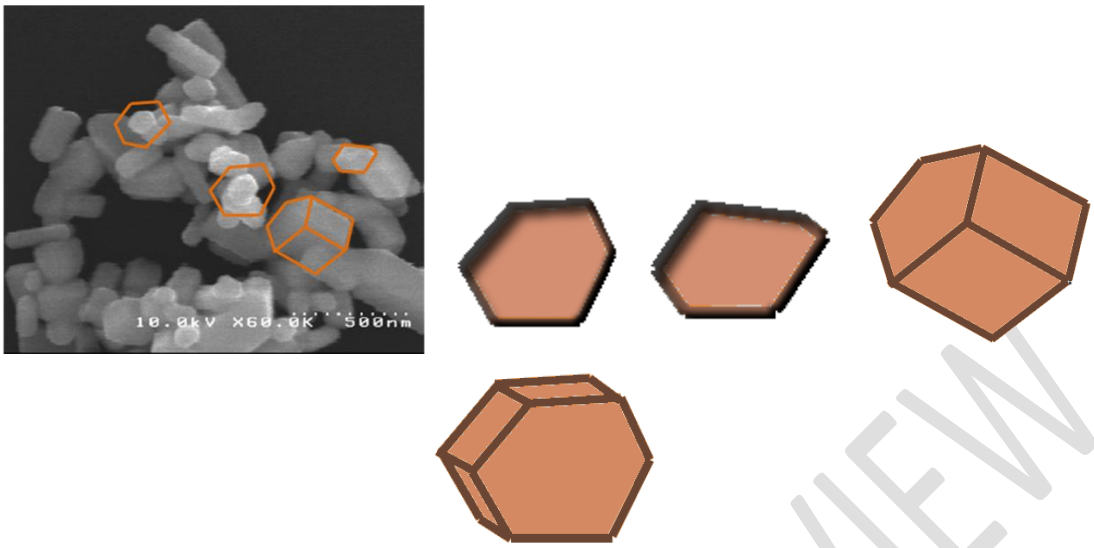

Fig. 5a. SEM image of Sn^{4+}:ZnO (1 Wt%)

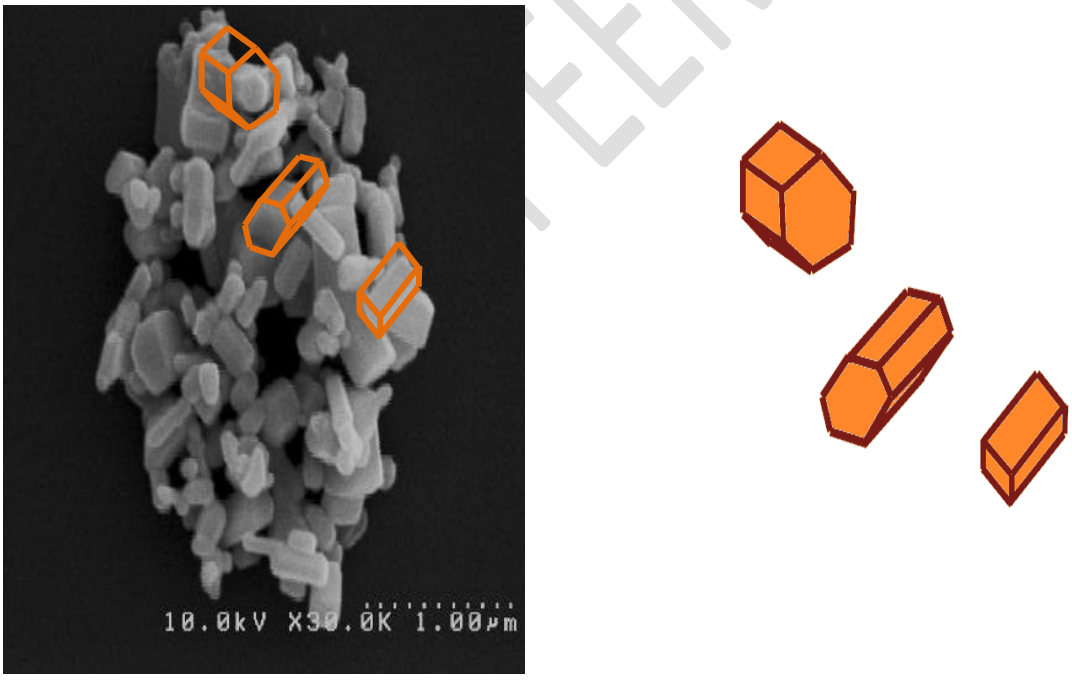

Fig. 5b. SEM image of Nd^{3+}:ZnO (1 Wt%)

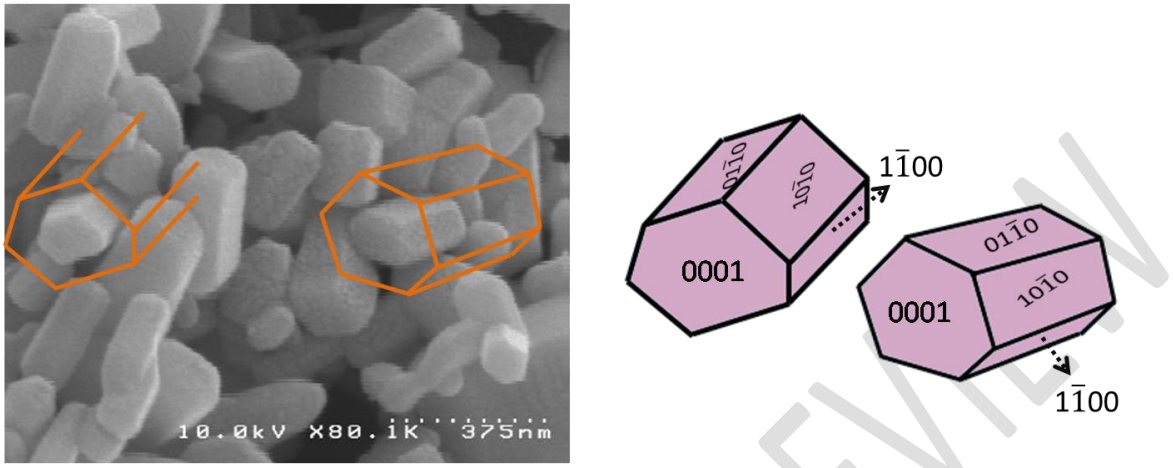

Fig. 5c. SEM image of In^{3+}:ZnO (1 Wt%)

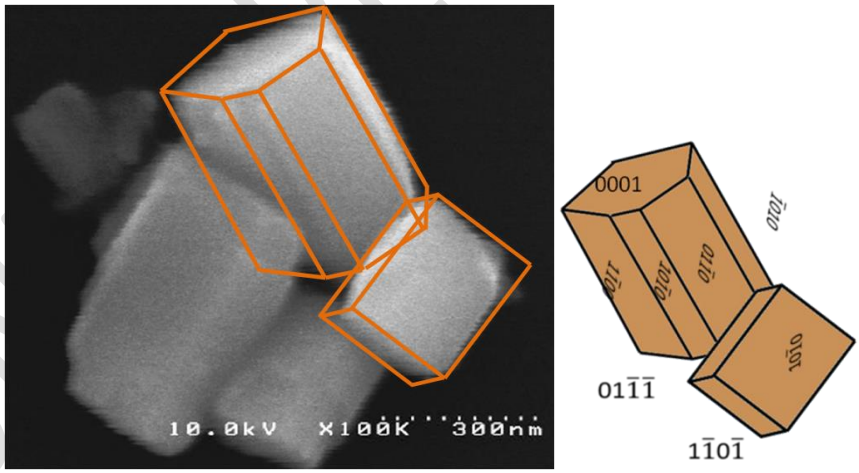

Fig. 5d. SEM image of Cr^{3+}:ZnO (1 wt%)

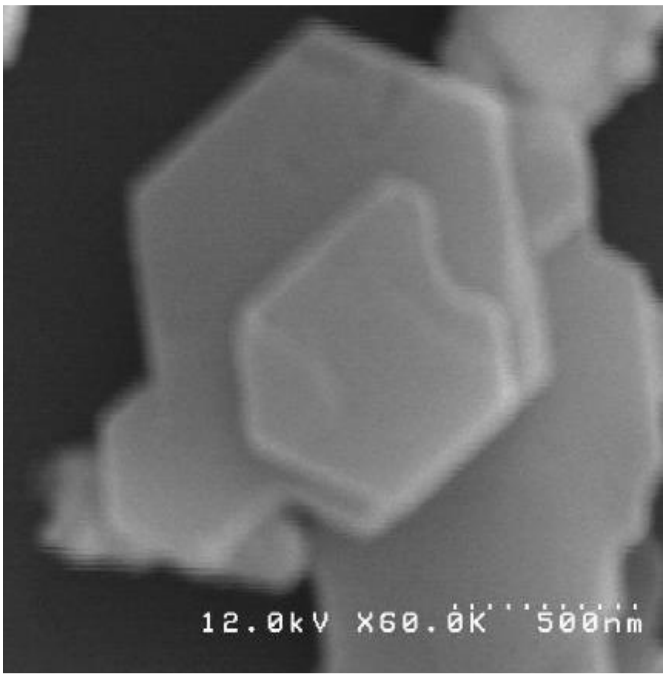

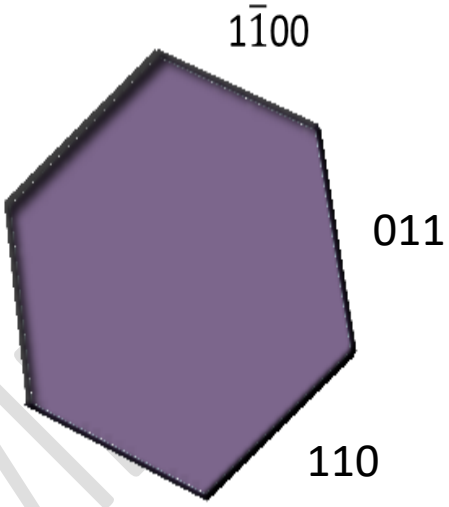

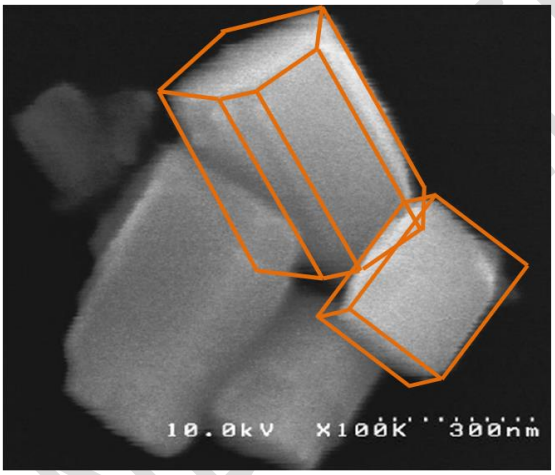

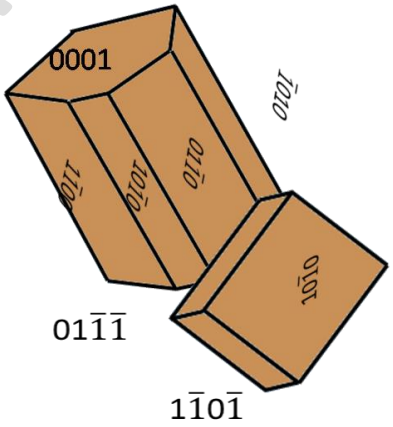

Fig. 5f. SEM image of Cd^{2+}:ZnO (1 Wt%)

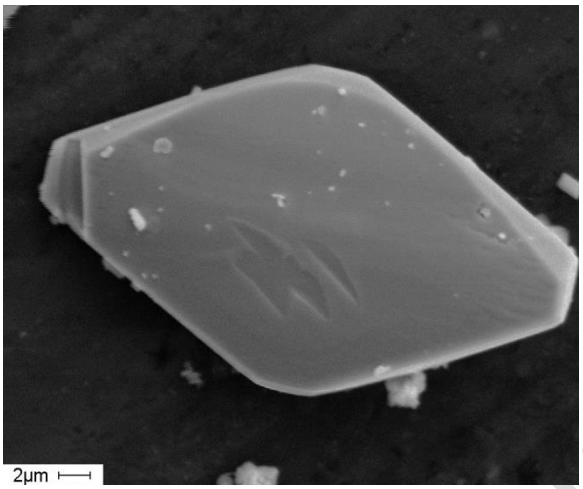

Fig. 5g. SEM image of Mo^{6+}:ZnO (1 Wt%)

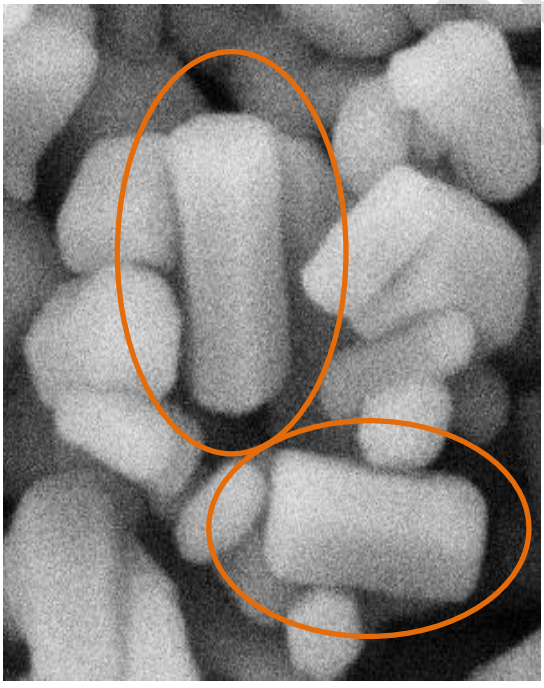

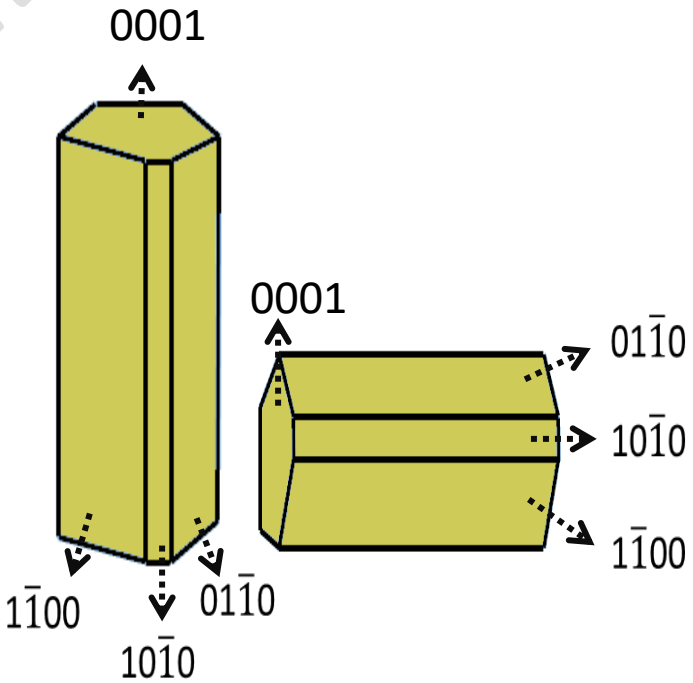

Fig. 5h. SEM image of 2M ZnO obtained with 2M ZnO raw material and caprylic acid surfactant

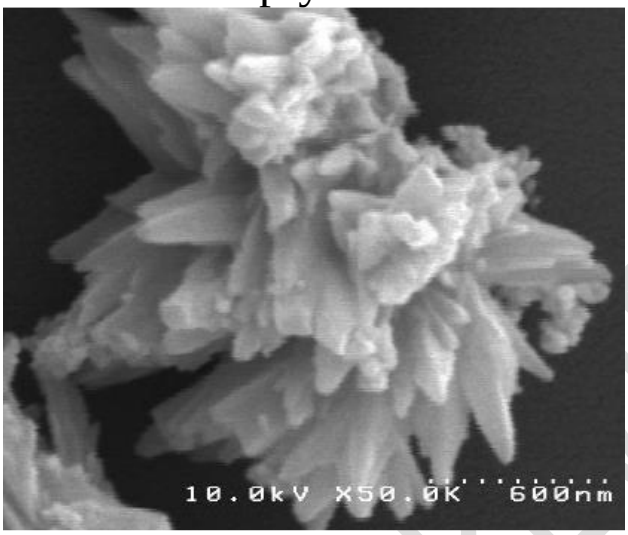

Fig. 5i. SEM image of Mo^{6+}:ZnO (excess Mo)

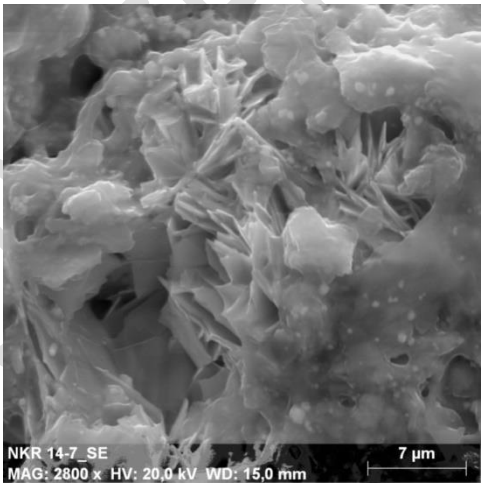

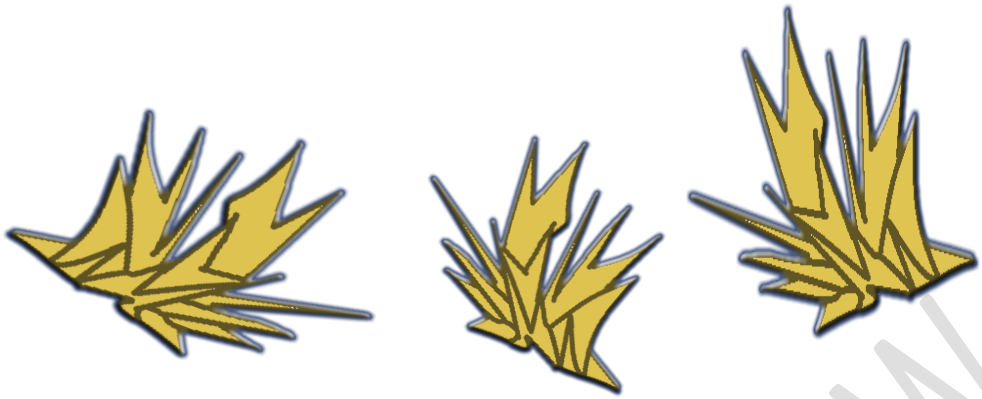

Fig. 5j. SEM image of 4M ZnO obtained with surplus 4M ZnO raw material and surfactant caprylic acid.

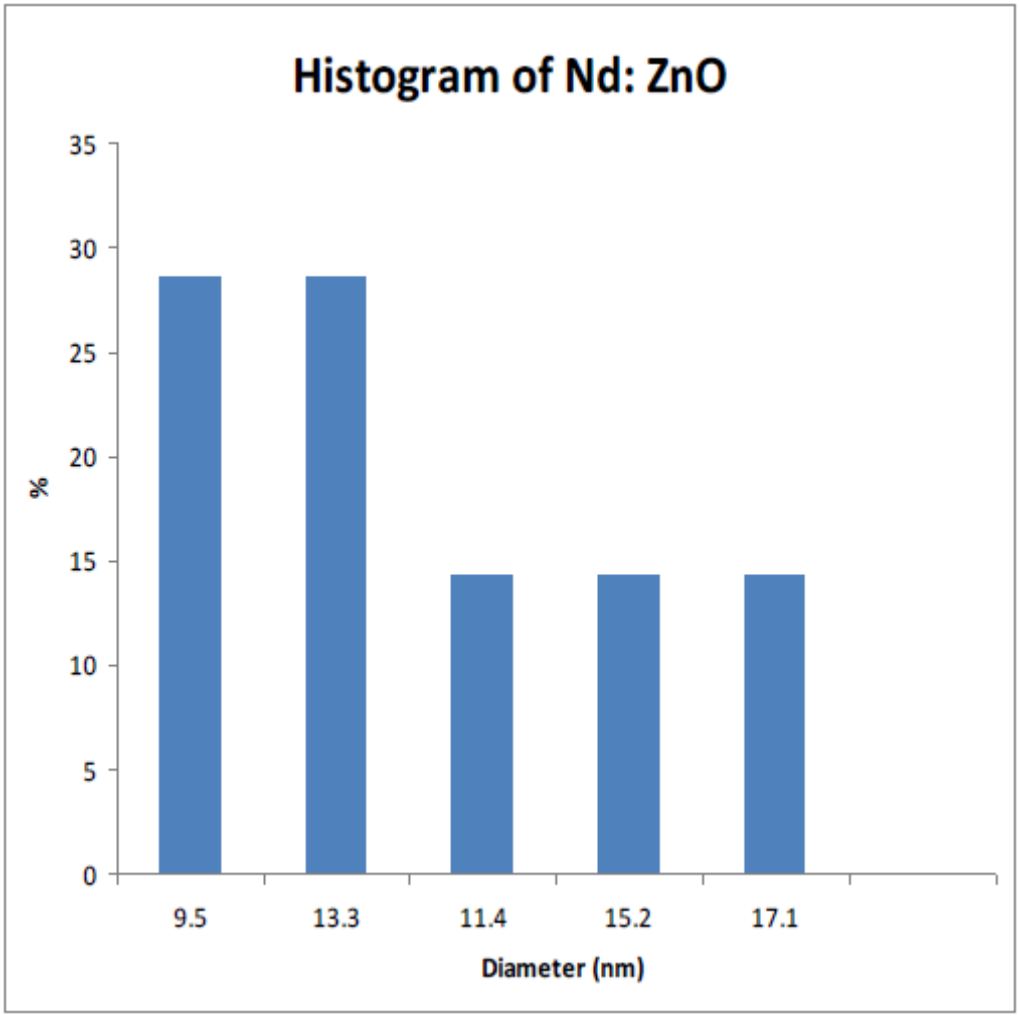

.

Fig. 6a. Particle size distribution in Nd^{3+}:ZnO

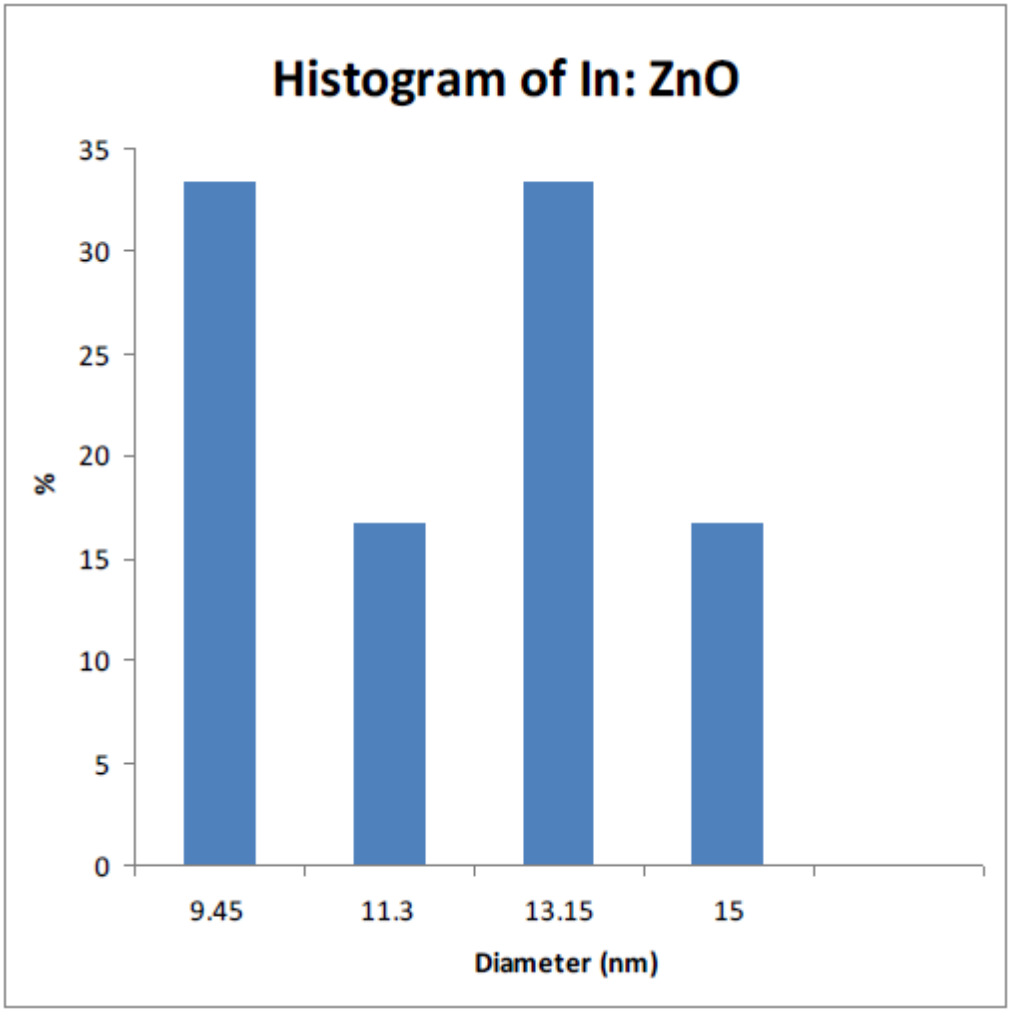

Fig. 6b. Particle size distribution in In^{3+}:ZnO

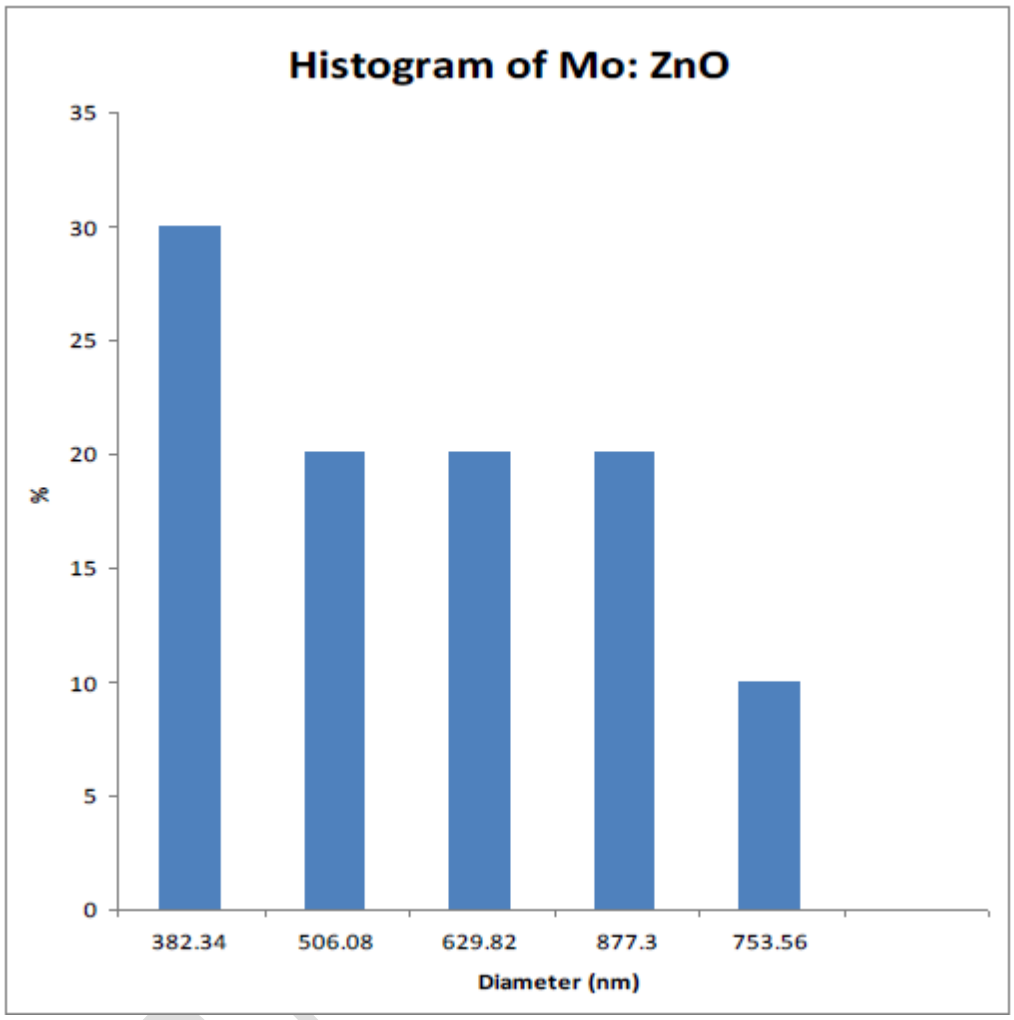

Fig. 6c. Particle size distribution in Mo^{6+}:ZnO

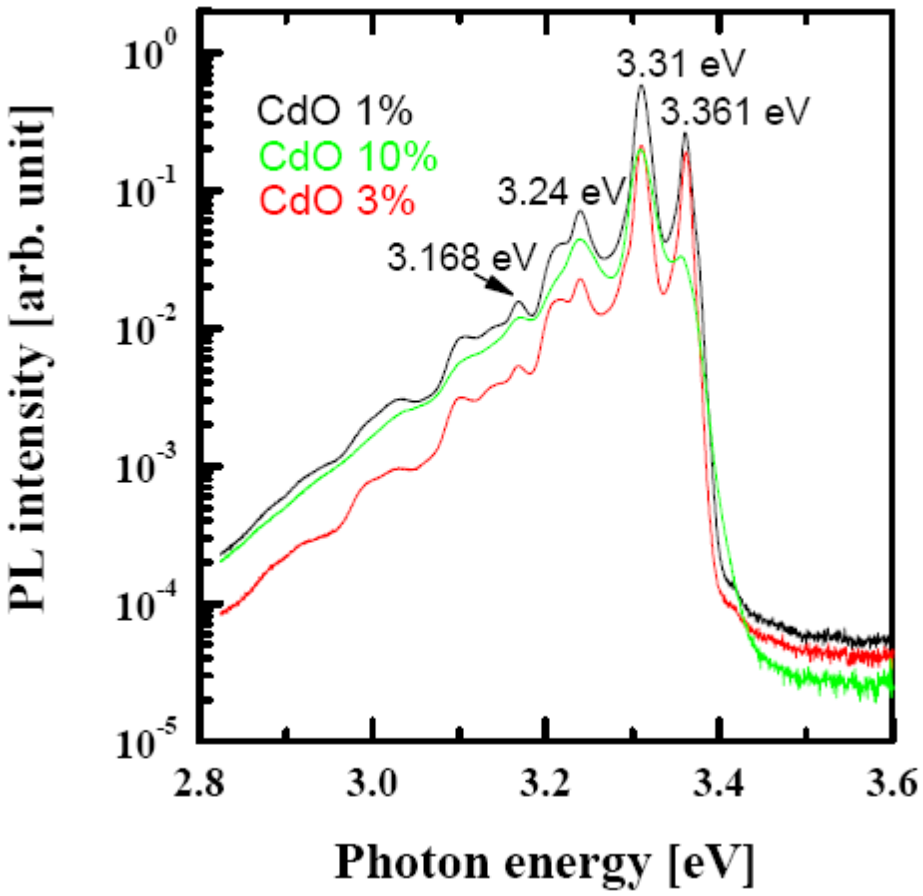

Fig.7a. Photoluminescence spectra of Cd^{2+} doped ZnO

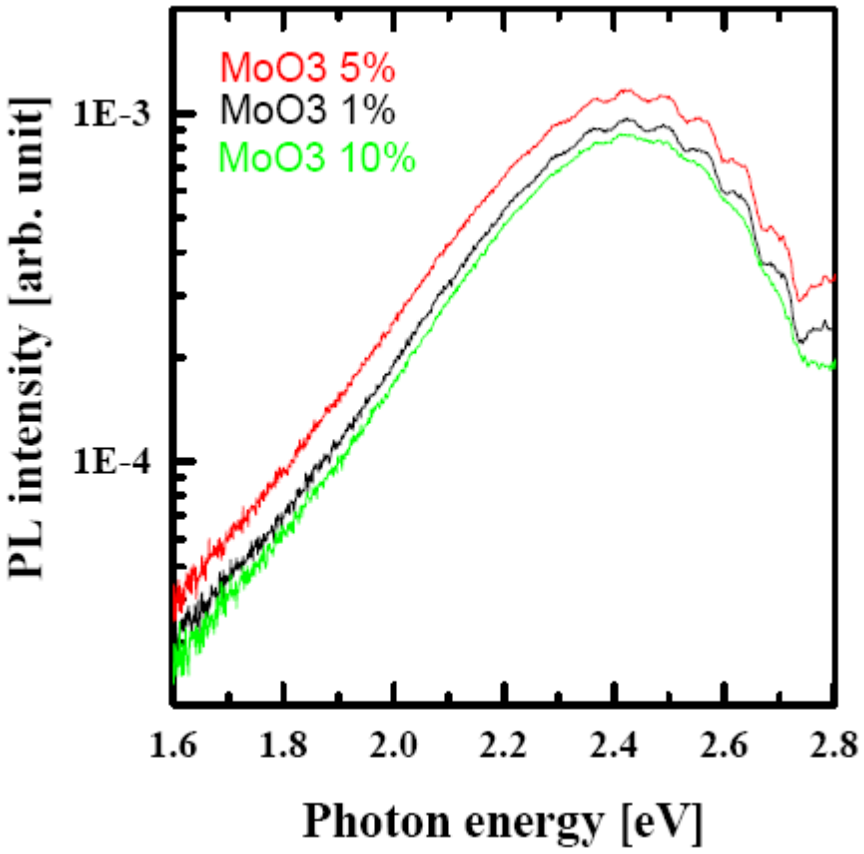

Fig. 7b. Photoluminescence spectra of Mo^{6+} doped ZnO

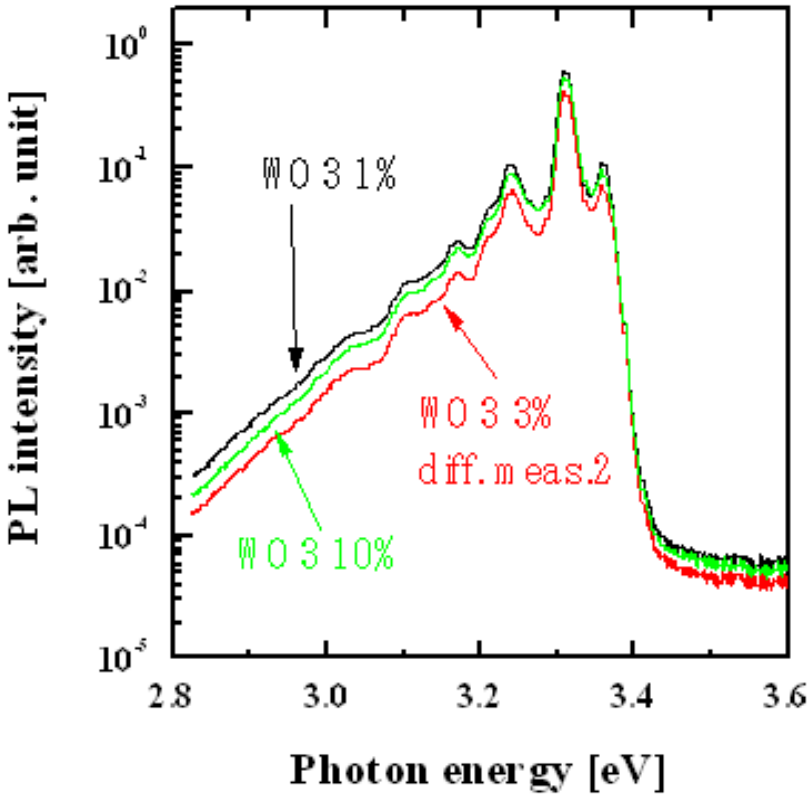

Fig. 7c. Photoluminescence spectra of W doped ZnO

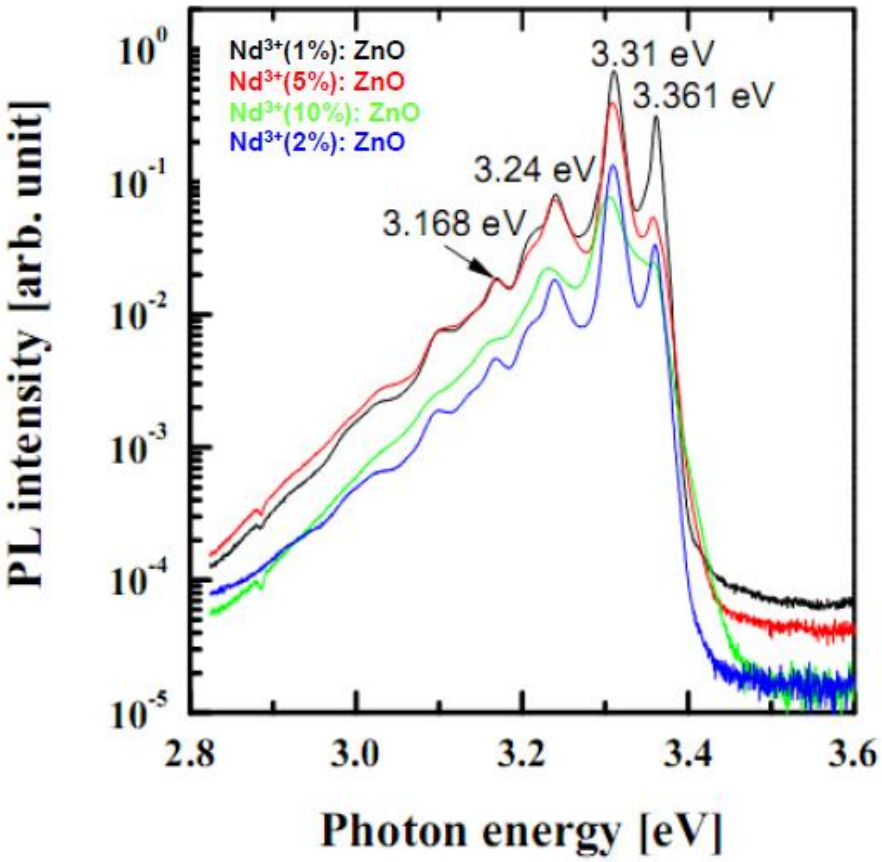

Fig. 7d. Photoluminescence spectra of Nd^{3+}:ZnO

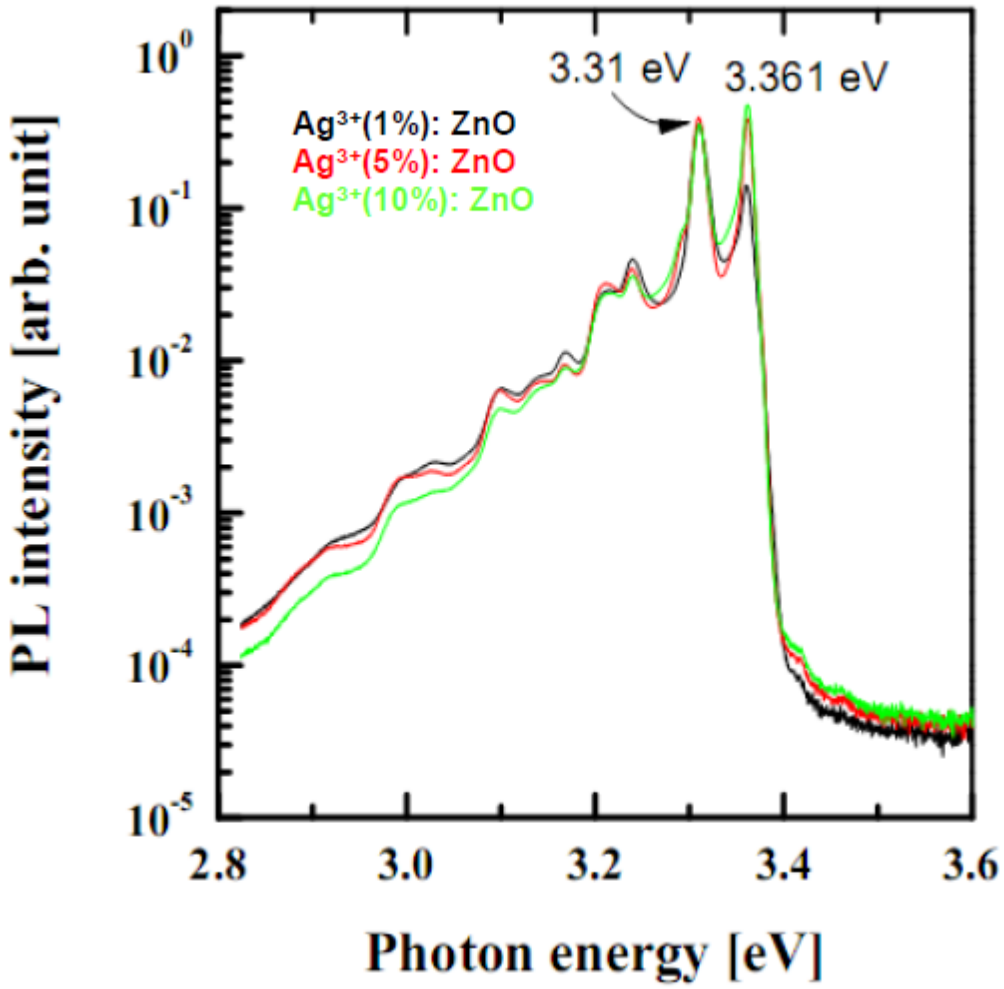

Fig. 7e. Photoluminescence spectra of Ag^{2+}:ZnO

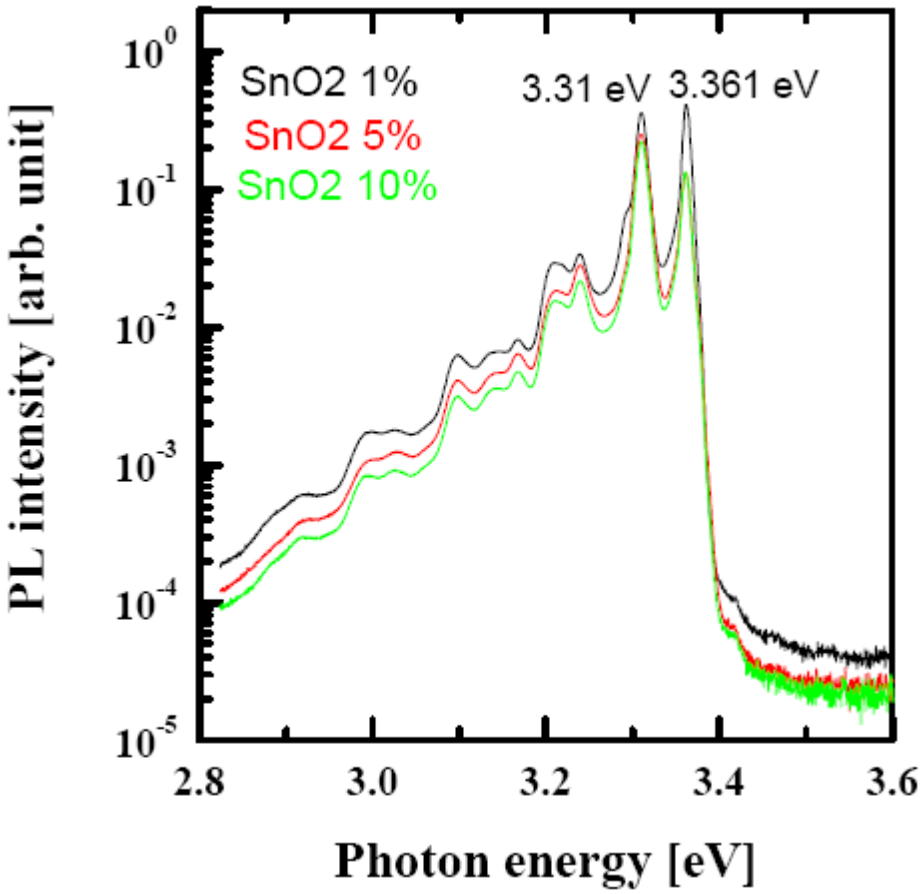

Fig. 7f. Photoluminescence spectra of Sn^{4+}:ZnO